

OAK RIDGE NATIONAL LABORATORY LIBRARIES



3 4456 0550191 7

cy. 1

TORUS WINDINGS WITH ASYMMETRIC MAGNET COILS

W. F. Gauster
P. L. Walstrom

OAK RIDGE NATIONAL LABORATORY
CENTRAL RESEARCH LIBRARY
DOCUMENT COLLECTION

LIBRARY LOAN COPY

DO NOT TRANSFER TO ANOTHER PERSON

If you wish someone else to see this
document, send in name with document
and the library will arrange a loan.

UCN-7969
(3 3-67)



OAK RIDGE NATIONAL LABORATORY
OPERATED BY UNION CARBIDE CORPORATION • FOR THE U.S. ATOMIC ENERGY COMMISSION

This report was prepared as an account of work sponsored by the United States Government. Neither the United States nor the United States Atomic Energy Commission, nor any of their employees, nor any of their contractors, subcontractors, or their employees, makes any warranty, express or implied, or assumes any legal liability or responsibility for the accuracy, completeness or usefulness of any information, apparatus, product or process disclosed, or represents that its use would not infringe privately owned rights.

Contract No. W-7405-eng-26

Thermonuclear Division

TORUS WINDINGS WITH ASYMMETRIC MAGNET COILS

W. F. Gauster and P. L. Walstrom

AUGUST 1973

NOTICE This document contains information of a preliminary nature and was prepared primarily for internal use at the Oak Ridge National Laboratory. It is subject to revision or correction and therefore does not represent a final report.

OAK RIDGE NATIONAL LABORATORY
Oak Ridge, Tennessee 37830
operated by
UNION CARBIDE CORPORATION
for the
U.S. ATOMIC ENERGY COMMISSION



3 4456 0550191 7



CONTENTS

	Page
I. Purpose of the New Winding Design	5
II. Wire-Wound Asymmetrical Coils (General Equation) . . .	6
III. Asymmetric Wire-Wound Circular Coils	8
A. Eccentric Circular Coils	8
B. Circular Coils with Flat Ends	9
C. Circular Coils with Two Flat Ends	10
IV. Asymmetric Bitter Coils	11
V. Discussion	15
References	17
Figure Captions	18
Figures	19

1

2

3

4

5

6

I. PURPOSE OF THE NEW WINDING DESIGN

For very large facilities, especially for fusion reactors, the use of superconducting windings seems to be mandatory. However, for machines of intermediate size it is difficult to make decisions between pulsed cryogenic and superconducting torus windings, considering expenses for the magnetic system including power supply and auxiliary parts, and taking into account the necessary development work.

For nonsuperconducting magnet systems, it is obviously important to design windings with minimum resistance and, therefore, reduced power demand. One possibility is to employ, instead of coils with the usual rectangular cross sections (Fig. 1a), wedge-shaped coils (Fig. 1b) which provide larger winding cross section. An example is the MIT "Alcator" machine, designed by D. B. Montgomery.^{1,2} A detailed discussion of torus windings with wedge-shaped coils has been presented by B. Oswald.² A disadvantage of such windings is the poor accessibility for particle injection and diagnostics. For tokamak experiments the free space inside the torus windings should be as large as possible in order to provide a sufficiently large flux area for ohmic heating. Therefore, the winding depth next to the torus axis should be as small as possible.

This paper discusses the idea of using asymmetric windings, which can be made relatively very thin at the inner side of the torus (toward the vertical torus axis), and of reducing the power demand by providing ample thickness toward the outside of the torus. Figure 2 shows three different examples of asymmetric coil shapes: (a) eccentric circular coils, (b) circular coils with flat ends (which use more effectively the winding space without interfering with the inside space of the torus),

and (c) coils with rectangular outside boundaries. It is possible to wind coils of Type (a) and (b) employing conductors of appropriate shape; however, also the Bitter-type design³ (helixes made up of plates) can be used.

In order to provide sufficient space for plasma diagnostics and particle injection, these asymmetric coils must not occupy the entire space around the torus. In the following, asymmetric coils with rectangular cross sections in the torus midplane are assumed (Fig. 3a). However, still smaller coil resistances could be achieved if toward the torus periphery the circumferential width of the coils is moderately increased; i.e., to such an extent that sufficiently free space is still available (Fig. 3b).

II. WIRE-WOUND ASYMMETRICAL COILS (GENERAL EQUATION)

We restrict our discussion here to asymmetrical coils with rectangular cross sections (i.e., with constant axial lengths) (Fig. 3a). In the case of a wire-wound coil, any distribution of the current density can be achieved by choosing appropriate variations in the wire cross sections.

Figure 4 shows the cross section of an asymmetric coil winding. We assume a constant axial thickness h (perpendicular to the cross section plane). The winding boundaries are characterized by the radii $r_a(\varphi)$ and $r_b(\varphi)$. By dividing the distances $r_b(\varphi) - r_a(\varphi)$ into a large number, n , of equal parts, we obtain n thin, nested coils with axial thickness h and with radial thicknesses varying from a/n to ka/n . We consider strip number p . The radial distance from the center O to the middle of the strip is

$$r_p(\varphi) = r_a(\varphi) + \left(p - \frac{1}{2}\right) \frac{[r_b(\varphi) - r_a(\varphi)]}{n}. \quad (1)$$

A short piece of strip number p , characterized by the differential $d\varphi$ of the angle φ , is shown in Fig. 5. The angle ψ_p between the axis of the wire element and the perpendicular to the radius vector r_p is determined by

$$\tan \psi_p = \frac{1}{r_p} \frac{dr_p}{d\varphi}. \quad (2)$$

The resistance of the wire element is

$$dR_p = \frac{\rho}{\lambda h} \frac{n}{(r_b - r_a) \cos \psi_p} \cdot \frac{r_p d\varphi}{\cos \psi_p} \quad (3)$$

where ρ stands for the resistivity of the conductor and λ for the packing factor of the winding. Combining Eqs. (2) and (3), we obtain

$$dR_p = \frac{\rho}{\lambda h} \frac{n}{r_b - r_a} \left[1 + \left(\frac{1}{r_p} \cdot \frac{dr_p}{d\varphi} \right)^2 \right] r_p d\varphi. \quad (4)$$

The resistance of strip number p is

$$R_p = 2 \int_{\varphi=0}^{\pi} dR_p, \quad (5)$$

and the total resistance is

$$R = \sum_{p=1}^n R_p. \quad (6)$$

It should be emphasized that the prescription used above is, of course, arbitrary. It seems to be the simplest way to define the conductor boundaries. However, with this very simple winding geometry, the magnitude and the direction of the current density \vec{j} vary with both r and φ . As is well known, a coil can be either wound in layers or in "pancakes." In the first case, helixes connected in series must be considered. In the second case, spirals are connected in series. However, the error caused by using simply the sum of the individual resistances of the strips, as considered by Eq. (6), is very small when n is the large number. Finally, we assumed for each strip an axial thickness h ; i.e., the axial thickness of the wire. If the total axial thickness of the coil is

$$l = mh, \quad (7)$$

Eq. (4) must be multiplied by m .

III. ASYMMETRIC WIRE-WOUND CIRCULAR COILS

We assume for the inner winding boundary

$$r_a(\varphi) = r_1 = \text{const.} \quad (8)$$

For the outer winding boundary we consider either eccentric circles (Fig. 2a) or circular coils with flat ends (Fig. 2b).

A. Eccentric Circular Coils

In Fig. 6 the distance $\overline{OO'}$ between the centers of the two eccentric circles is b ; the radius of the outer circle is r_2 . Thus,

$$b = \frac{k-1}{2} a, \quad (9)$$

and

$$r_b = -b \cos \varphi + r_2 \sqrt{1 - (b/r_2)^2 \sin^2 \varphi}. \quad (10)$$

Equations (8) and (10) can be used to evaluate Eqs. (1) to (6). For a concentric circular coil winding (where $k = 1$, $b = 0$, and $r_b = r_2 = r_1 + a$), the resistance is obviously

$$R_o = \frac{\pi \rho (2 r_1 + a)}{\lambda h a}. \quad (11)$$

For the eccentric circular coil windings, the ratio R_o/R depends on the values of k and r_1/a . In order to calculate the R_o/R values shown in Fig. 7, Eqs. (4) and (5) were integrated numerically with 50 radial increments and 100 increments in the azimuthal angle φ . It can be proved by means of an analytical integration that

$$\lim_{\frac{r_1}{a} \rightarrow \infty} \frac{R_o}{R} = \sqrt{k}. \quad (12)$$

B. Circular Coils with Flat Ends

The winding configuration is shown in Fig. 8. The shape is an annular ring of radial winding thickness ka , cut off on one side by a vertical cut ABC at a distance $r_1 + a$ from the center O. The angle φ_o is determined by

$$\cos \varphi_0 = \frac{r_1 + a}{r_1 + ka} \quad (13)$$

For small k (say $k < 5$), the $\cos^2 \psi$ term in Eq. (3) can be neglected and the integration over the area ABCDEA can be performed analytically.⁴ The calculation of the resistance contribution over the concentric ring sector ACDEA is trivial.

The general case, where the $\cos^2 \psi$ factor must be considered, has been solved using the previously described "strip method" with $n = 100$ and also with 100 steps in the azimuthal angle φ for the numerical integration of Eqs. (4) and (5). It is easy to prove that in the case of circular coils with flat ends.

$$\lim_{\left. \begin{array}{l} \frac{R_0}{R} \\ \frac{r_1}{a} \rightarrow \infty \end{array} \right\}} = k \quad (14)$$

The numerical results for various (r_1/a) -values are represented in Fig. 9. As can be seen, for the lower values of r_1/a , the resistance ratio reaches a maximum in the k range shown in Fig. 9. It can be easily shown that, in the limit $k \rightarrow \infty$, for any constant value of r_1/a , R_0/R approaches zero. This means that for any r_1/a value, R_0/R must reach a maximum for some k and then decrease as k increases.

C. Circular Coils with Two Flat Ends

In order to provide space for neutral beam injection, it may be necessary to use coils that are cut off on both ends. The second cut is made on the side of the coil opposite to the first cut at a distance $r_1 + k'a$ from the center.

The resistance ratio R_o/R was calculated for coils with $r_1/a = 3.48$ and with K values of 3 and 4, for K' values ranging from zero to K . The results of this calculation and the coil configuration itself are shown in Fig. 10.

IV. ASYMMETRIC BITTER COILS

In the following we restrict ourselves to the calculation of the ohmic resistance of eccentric, circular Bitter coils. From conformal mapping, the case of bipolar circles (Fig. 11) corresponding to the complex function

$$\frac{z}{z_0} = \frac{(e^w + 1)}{e^w - 1} \quad (15)$$

is well known.⁵ Two families of circles which intersect each other with an angle of $\pi/2$ can be considered as equipotential and flow lines, respectively. The scalar potential V satisfies Laplace's equation

$$\nabla^2 V = 0 . \quad (16)$$

If we restrict ourselves to the upper half plane (in order to make the potential single valued), the current density \vec{J} of a current flowing through a plate of uniform thickness h and uniform resistivity ρ can be written as

$$\vec{J} = -\frac{1}{\rho} \nabla V . \quad (17)$$

The boundaries of an eccentric circular Bitter plate are two circular flow lines C_1 and C_2 ; the equipotential lines are circles with the centers

O' located on the straight line G (Fig. 12). We use a bipolar coordinate system (with $|\overline{OO_1}| = |\overline{OO_2}| = m$), so that the location of any point P is determined by the angle α and the ratio

$$\frac{r_1}{r_2} = \beta . \quad (18)$$

In Cartesian coordinates

$$\tan \alpha_1 = \frac{y}{x - m} \quad (19)$$

$$\tan \alpha_2 = \frac{y}{x + m} . \quad (20)$$

Therefore, the angle $(O_1 - P - O_2)$ is equal to

$$\alpha = \alpha_1 - \alpha_2 = \tan^{-1} \left(\frac{2my}{x^2 + y^2 - m^2} \right) . \quad (21)$$

Figure 13 shows the intersections x_1 and x_1' of the $\beta_1 = \text{constant}$ flow line with the abscissa axis and the corresponding points x_2 and x_2' for $\beta_2 = \text{constant}$. From Eq. (18) it follows that

$$\frac{x_1 - m}{x_1 + m} = \frac{m - x_1'}{m - x_1'} . \quad (22)$$

A similar equation also holds for x_2 and x_2' . We introduce

$$r = \frac{x_1 - x_1'}{2} , \quad (23)$$

$$a = x_1' - x_2' , \quad (24)$$

and

$$ka = x_2 - x_1 . \quad (25)$$

We designate the resistance of the upper half of the eccentric, circular Bitter coil with $R/2$; and we assume on the surface with the cross section area $(x_2 - x_1)h$, the potential $V = V_0$, and on the surface with the cross section area $(x'_1 - x'_2)h$, the potential $V = 0$. The current I flowing through the upper half of the Bitter coil is

$$I = h \int_{x_1}^{x_2} J \Big|_{y=0} dx , \quad (26)$$

and because of Eq. (17)

$$J \Big|_{y=0} = - \frac{1}{\rho} \frac{dV}{dy} \Big|_{y=0} . \quad (27)$$

For $V = V_0$, the bipolar coordinate α is

$$\alpha_0 = 0 , \quad (28)$$

for $V = 0$,

$$\alpha'_0 = \pi . \quad (29)$$

Thus,

$$V = V_0 \left(1 - \frac{\alpha}{\pi} \right) . \quad (30)$$

From Eq. (8) it follows that

$$\alpha = \tan^{-1} \frac{2my}{x^2 + y^2 - m^2} , \quad (31)$$

from Eqs. (2) and (19)

$$J \Big|_{y=0} = \frac{V_0}{\pi \rho} \cdot \frac{2m}{x^2 - m^2}, \quad (32)$$

and, finally,

$$I = \frac{V_0 h \lambda}{\pi \rho} \ln \frac{(x_1 + m)(x_2 - m)}{(x_1 - m)(x_2 + m)}. \quad (33)$$

Therefore the resistance of a circular, eccentric Bitter coil is

$$R = \frac{2V_0}{I} = \frac{2\pi\rho}{h\lambda \ln \frac{(x_1 + m)(x_2 - m)}{(x_1 - m)(x_2 + m)}}. \quad (34)$$

Considering Eq. (11),

$$\frac{R_0}{R} = \frac{2r + a}{2a} \ln \frac{(x_1 + m)(x_2 - m)}{(x_1 - m)(x_2 + m)}. \quad (35)$$

Introducing normalized coordinates

$$\xi_1 = \frac{x_1}{m} \quad \text{and} \quad \xi_2 = \frac{x_2}{m}, \quad (36)$$

we obtain

$$\frac{R_0}{R} = \frac{2r + a}{2a} \ln \frac{(\xi_1 + 1)(\xi_2 - 1)}{(\xi_1 - 1)(\xi_2 + 1)}. \quad (37)$$

Finally, it can be shown that

$$\xi_1 = \left[k \frac{2 \left(\frac{r}{a} \right) + 1}{2 \left(\frac{r}{a} \right) + k} \right]^{1/2} \quad (38)$$

and

$$\xi_2 = \frac{k}{\xi_1} = \left[k \frac{2 \left(\frac{r}{a} \right) + k}{2 \left(\frac{r}{a} \right) + 1} \right]^{1/2}. \quad (39)$$

Using Eqs. (37), (38), and (39) the resistances of eccentric, circular Bitter coils can be calculated.

Example:

$$m = 3; \quad x_1 = 4.5; \quad x_2 = 6; \quad \xi_1 = 1.5; \quad \xi_2 = 2$$

$$r = 1.25; \quad a = 0.5; \quad r/a = 2.5; \quad k = 3; \quad R_o/R = 1.533$$

From L'Hopital's rule it follows that in the limit $r/a \rightarrow \infty$ (e.g., the winding depth approaches zero while the inner radius of the windings remains constant), the ratio R_o/R approaches the value \sqrt{k} . This limit is the same as that derived from eccentric circular wire-wound coils [Eq. (12)], as one would expect. It is clear that significant differences in resistance ratio between wire-wound and Bitter eccentric circular coils will become apparent only for small values of r/a . For this reason, a short computer program was written to evaluate Eq. (37) over a matrix of values of k and r/a .

The results of the comparison are shown in Fig. 14, where the ratio of the resistance ratios for Bitter-type and wire-wound coils is plotted vs k .

V. DISCUSSION

As far as we know, no detailed calculation concerning the reduction of the resistance of torus windings by providing asymmetric coils has

yet been made. For another purpose, namely to change the shape of the magnetic field, asymmetric coils have been designed and the technology of manufacturing such coils has been carefully investigated for the ORNL "Bumpy Torus" Project by J. N. Luton.⁶ However, these two mentioned purposes require very different approaches.

For the ORNL "ORMAK" Project⁷ (Fig. 1a), $r_1 = 13.1$ in., $r_2 = 14.7$ in., and $r_3 = 31.6$ in.; $\delta = 31.6/13.1 = 2.41$, $\alpha = 14.7/13.1 = 1.12$, and the resistance R_o of the rectangular coils to the resistance R of the wedge-shaped coils is (compared appendix to Ref. 2, pages I and II)

$$\frac{R_o}{R} = \frac{\sqrt{\delta^2 - \left(\frac{1 + \alpha}{2}\right)^2}}{\delta - \alpha} = 1.6 . \quad (40)$$

The family of curves in Fig. 9 shows that much higher resistance ratios could be easily achieved using concentric circular coils with flat ends. For instance, if we assume a winding thickness of $ka = 4 \times 1.6$ in. = 6.4 in. at the outside periphery of the torus, the resistance ratio $R_o/R = 2.5$ could be achieved. If the winding thickness at the outside of the torus could be made still larger than 6.4 in., even better resistance ratios could be obtained. However, it should be emphasized that the main advantage of the asymmetric coils is the better accessibility to the interior of the torus.

We acknowledge discussions with several of our colleagues, especially with H. M. Long and J. N. Luton, Jr.

REFERENCES

1. Bruno Coppi and Jan Remi, "The Tokamak Approach in Fusion Research," Sci. Am. 227, 65-75 (July 1971).
"Design of Alcator - The MIT High Field Torus," IV European Conference on Controlled Fusion and Plasma Physics (Rome, Italy, August 31-September 4, 1970) p. 20.
Progress Report, Francis Bitter National Magnet Laboratory, July-December 1971, MIT-NML-PR-71/2, p. 117.
2. B. Oswald, "Berechnungsgrundlagen, Optimierung und Kostfaktoren normalleitender Kryotechnischer und Supraleitender Magnete für die experimentelle Plasmaphysik," Max-Planck Institut für Plasmaphysik Report No. IPP 4/96 (November 1971).
3. F. Bitter, Rev. Sci. Instr. VII, 479-487 (1936); VIII, 318-319 (1937); IX, 373-381 (1939).
4. ORNL, Engineering Sciences Memo No. 82 (August 23, 1972).
5. See for instance, P. Moon and D. E. Spenser, Field Theory Handbook (Springer Verlag, Berlin, 1961).
6. Thermonuclear Division Annual Progress Report for Period Ending December 31, 1971, ORNL-4793, p. 52.
7. Thermonuclear Division Annual Progress Report for Period Ending December 31, 1970, ORNL-4688, pp. 44-66.

FIGURE CAPTIONS

- Figure 1 Torus windings.
- Figure 2 Asymmetric coil shapes.
- Figure 3 Tori with asymmetric coils.
- Figure 4 Asymmetric coil winding.
- Figure 5 Winding element.
- Figure 6 Circular eccentric coil.
- Figure 7 Resistance ratios of circular eccentric coils.
- Figure 8 Circular coil with flat end.
- Figure 9 Resistance ratios of circular flat end coils.
- Figure 10 Resistance ratios for double flat end coils.
- Figure 11 Families of orthogonally intersecting circles.
- Figure 12 Bipolar coordinate system.
- Figure 13 Coordinates used for resistance calculation of eccentric
circular Bitter coil.
- Figure 14 Comparison of resistance ratios of eccentric circular
Bitter-type and wire-wound coils.

ORNL-DWG 72-11622R

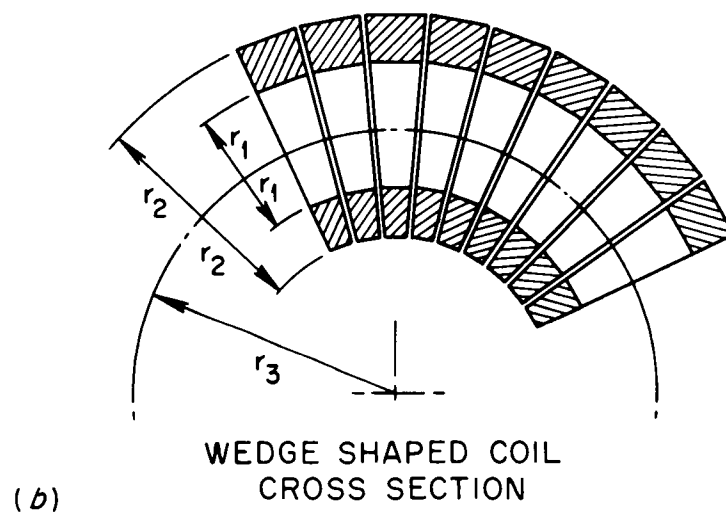
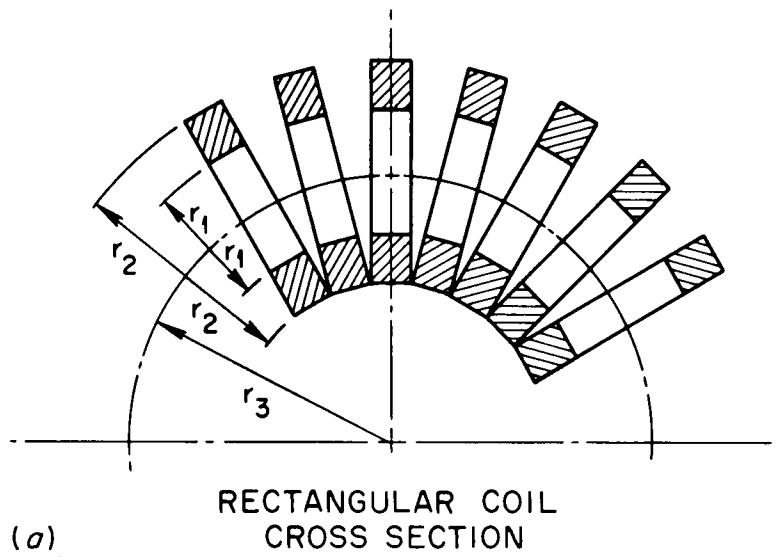
TORUS WINDINGS

FIGURE 1

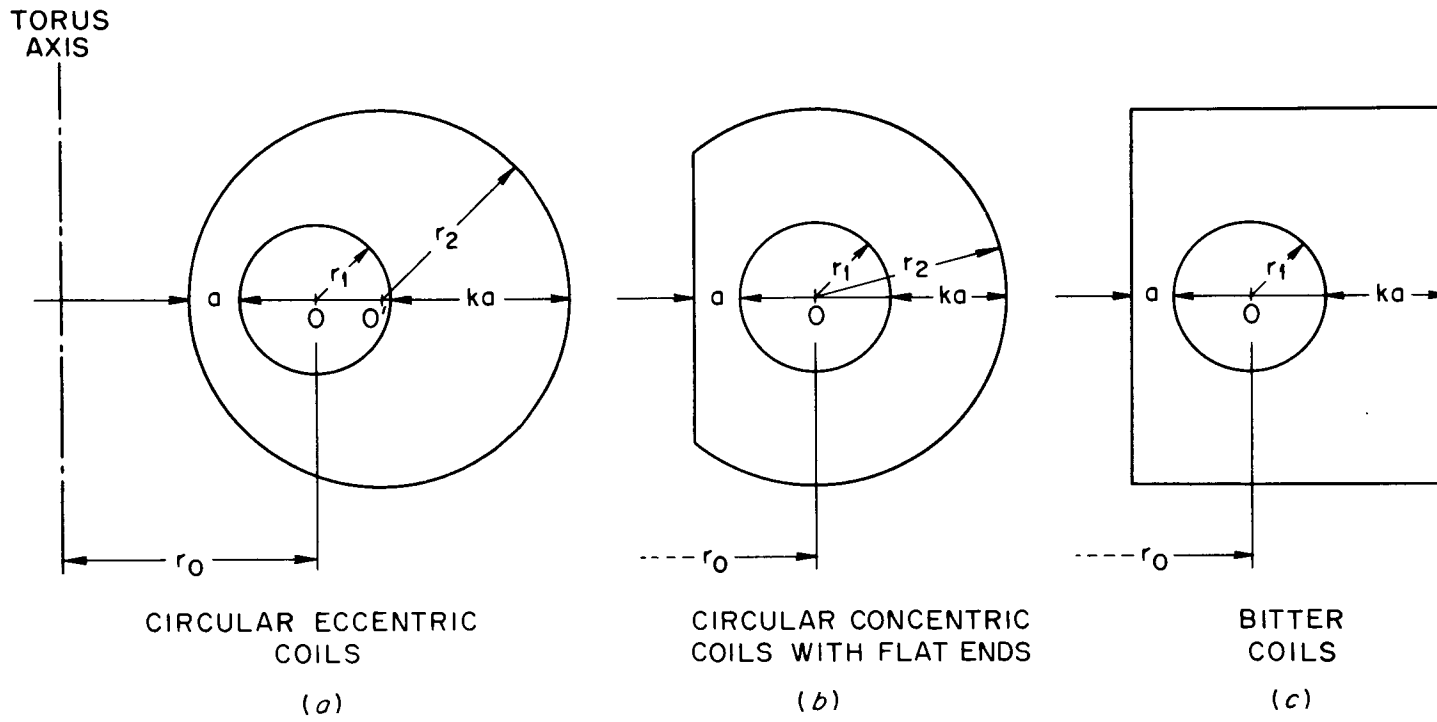
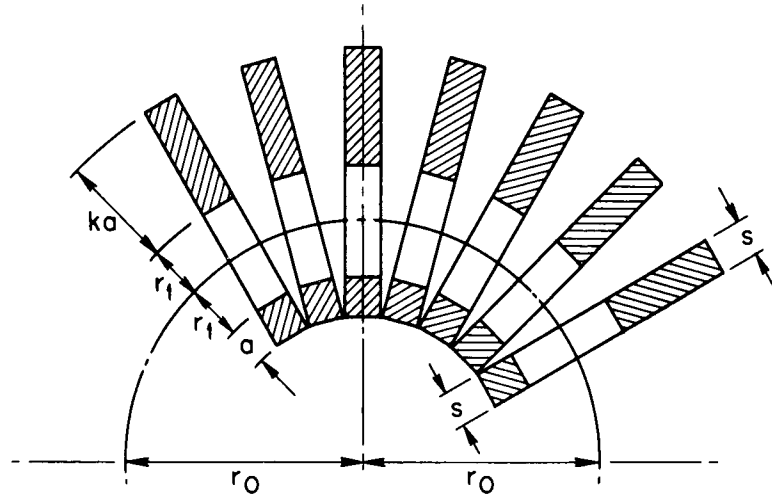
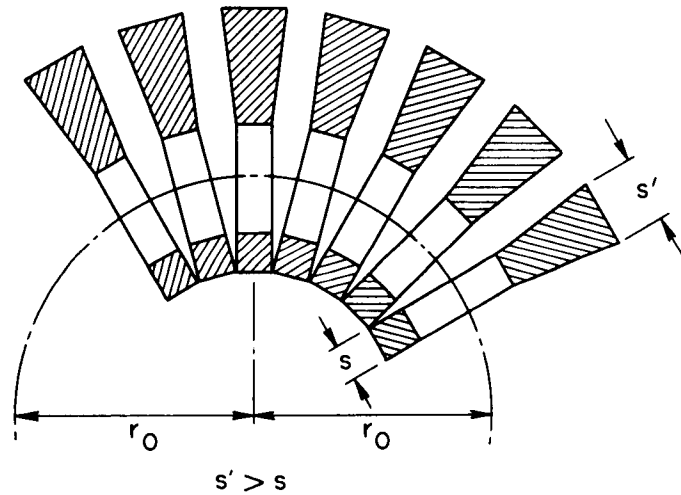


FIGURE 2

TORI WITH ASYMMETRIC COILS
(PLAN VIEW)



(a) CONSTANT AXIAL WIDTH
OF COIL WINDINGS



(b) VARIABLE AXIAL WIDTH
OF COIL WINDINGS

FIGURE 3

ORNL-DWG 72-11625R

ASYMMETRIC COIL WINDING

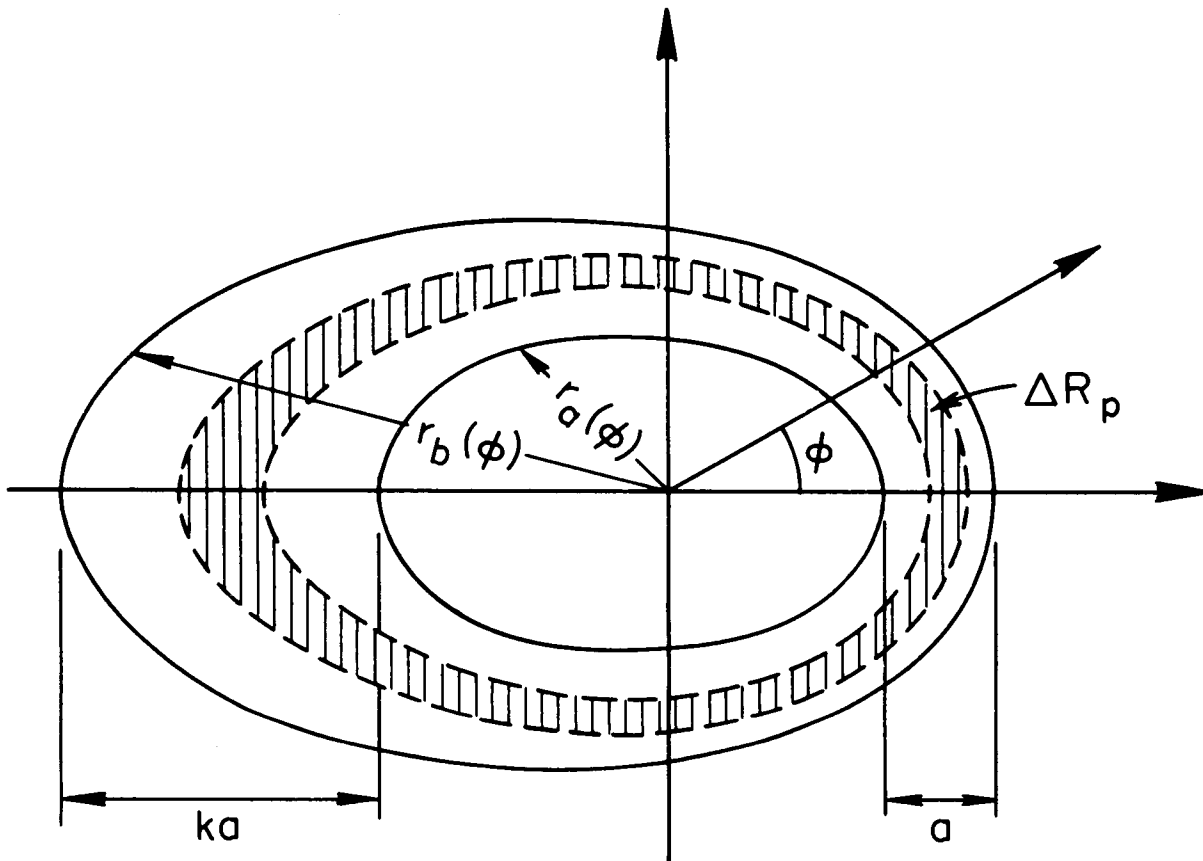


FIGURE 4

ORNL-DWG 73-4852

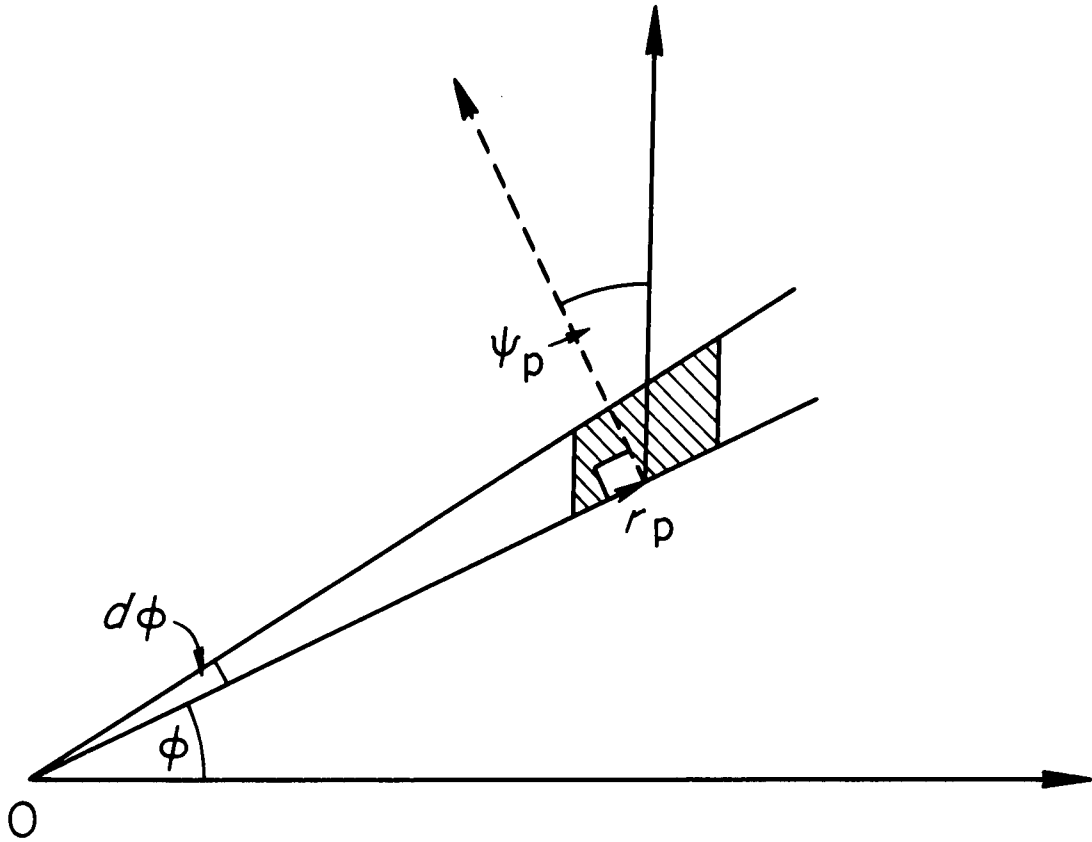
Short Piece of Strip Number ρ

FIGURE 5

ORNL-DWG 73-4853

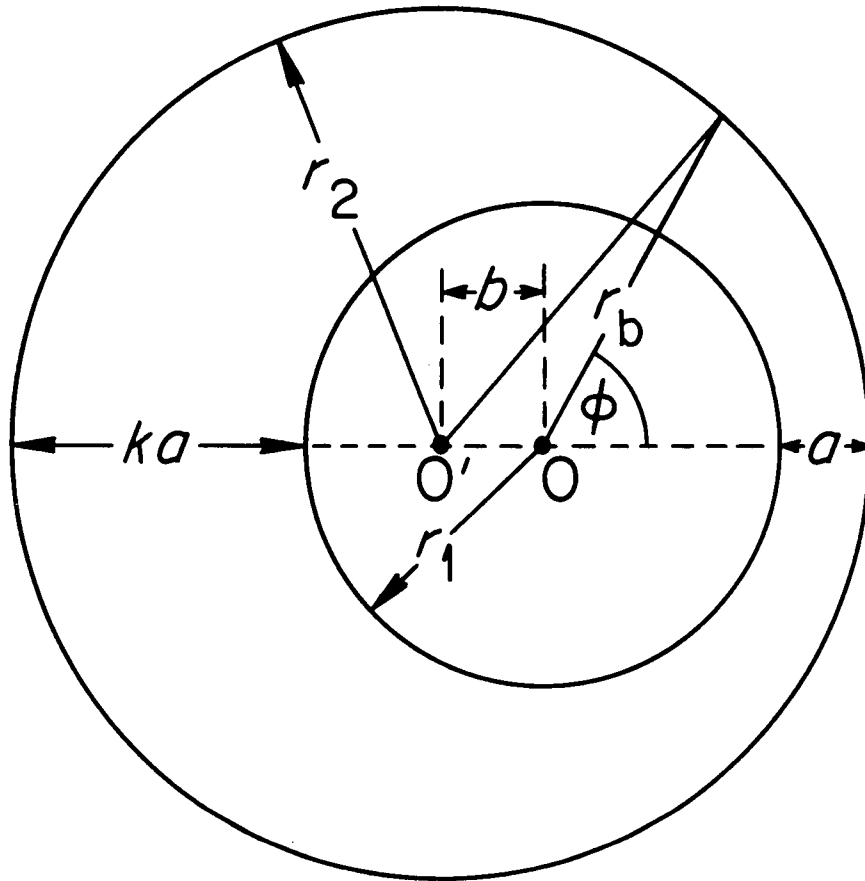
**Circular Eccentric Coil**

FIGURE 6

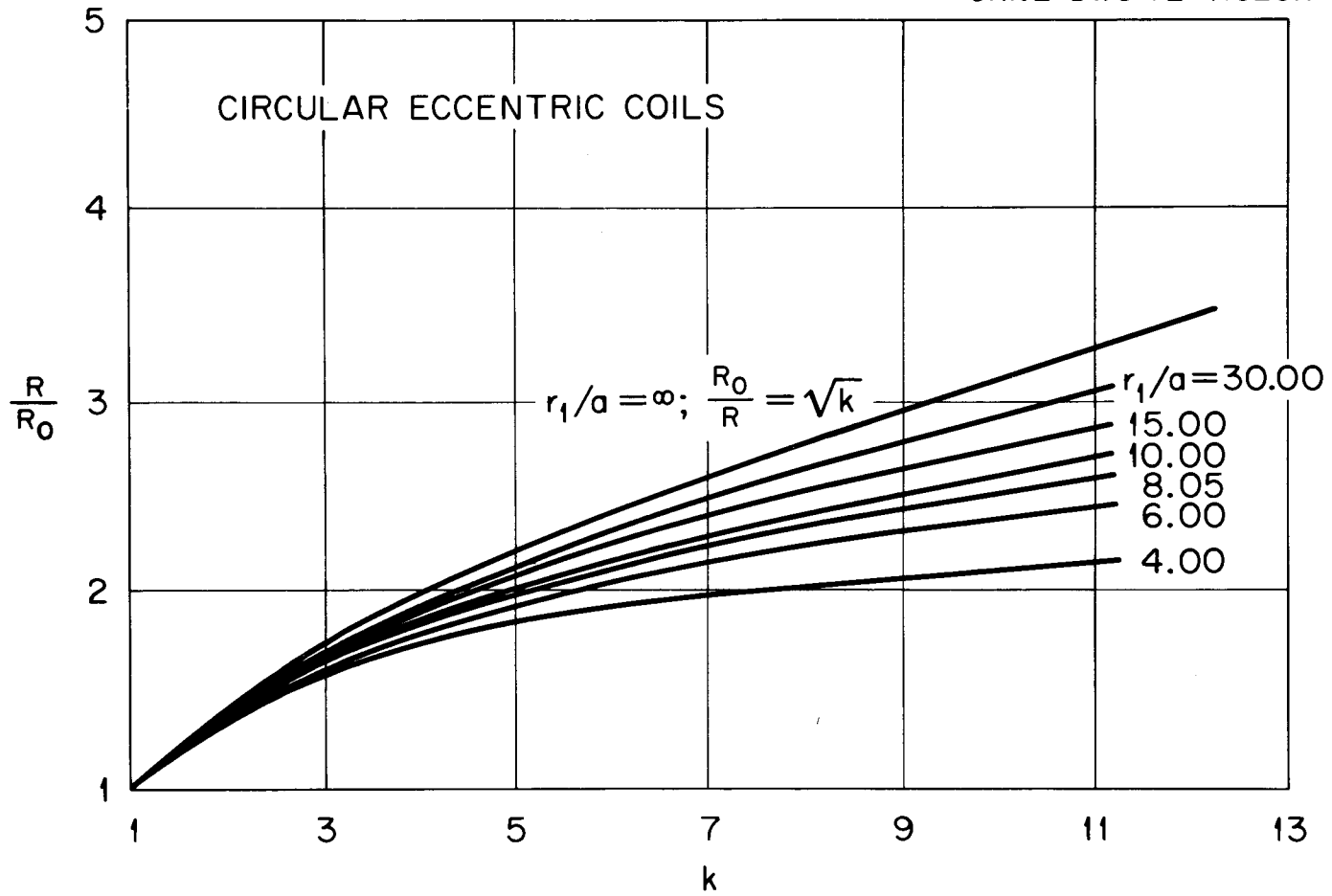
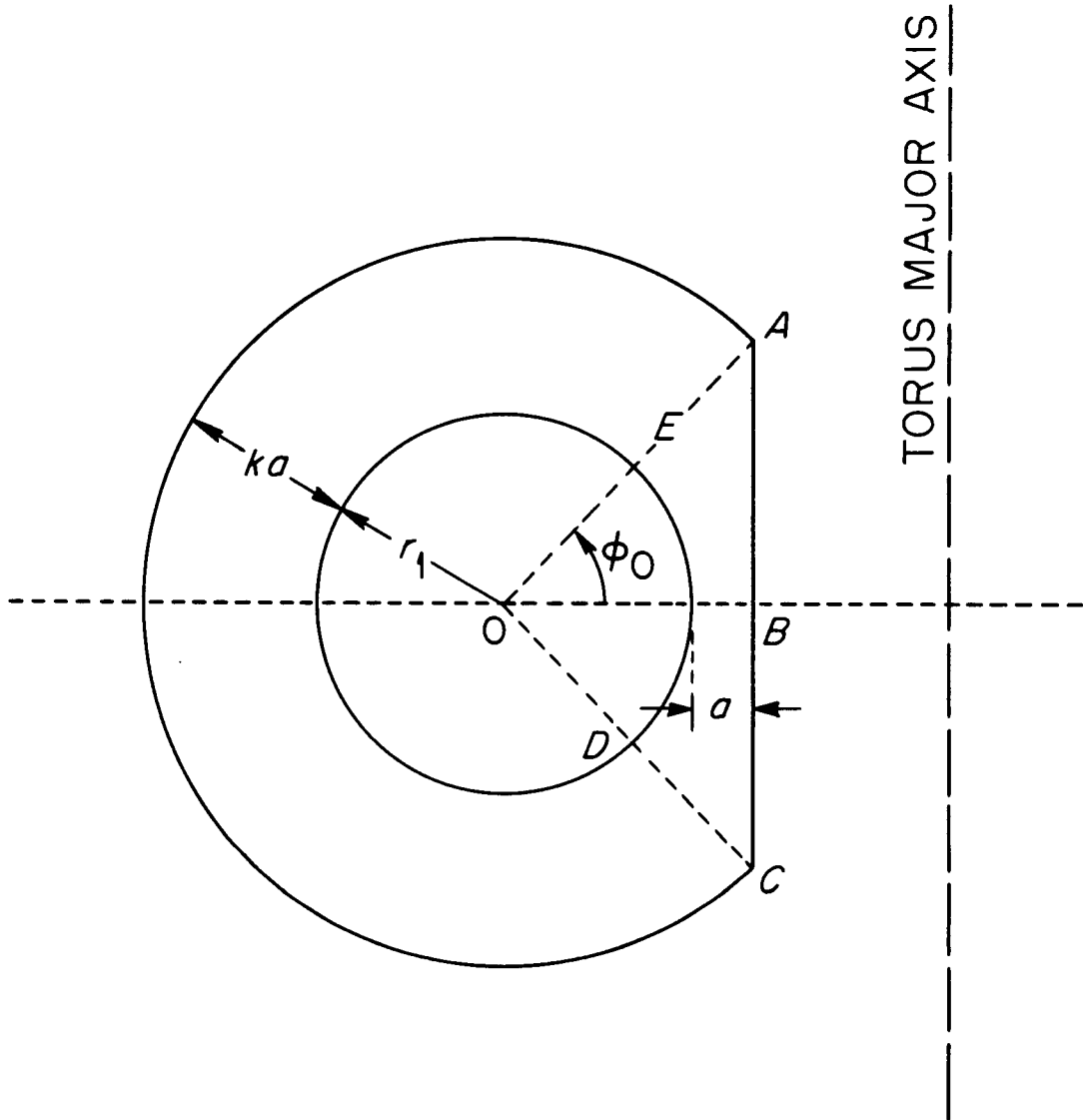


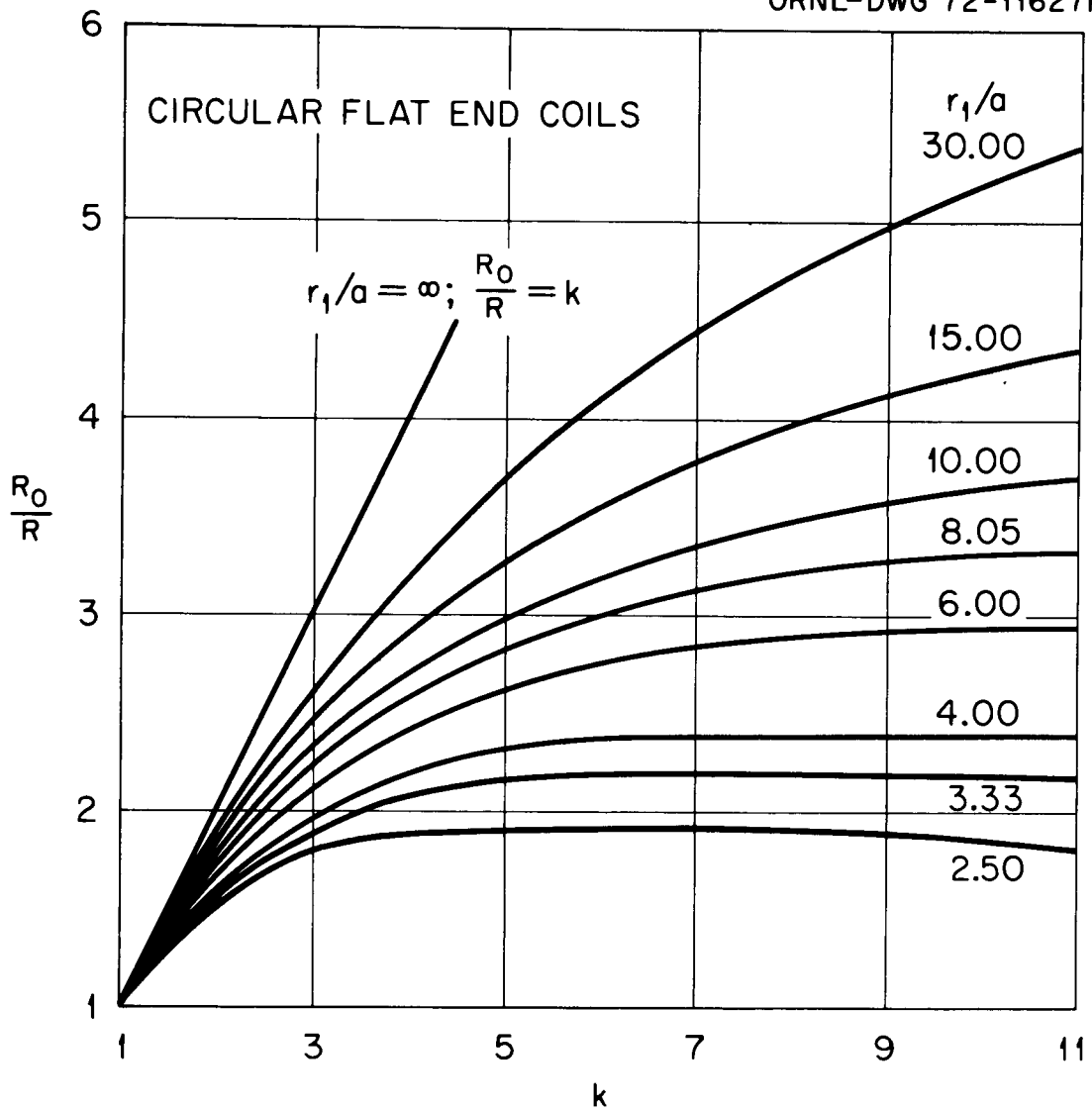
FIGURE 7



Circular Flat End Coil

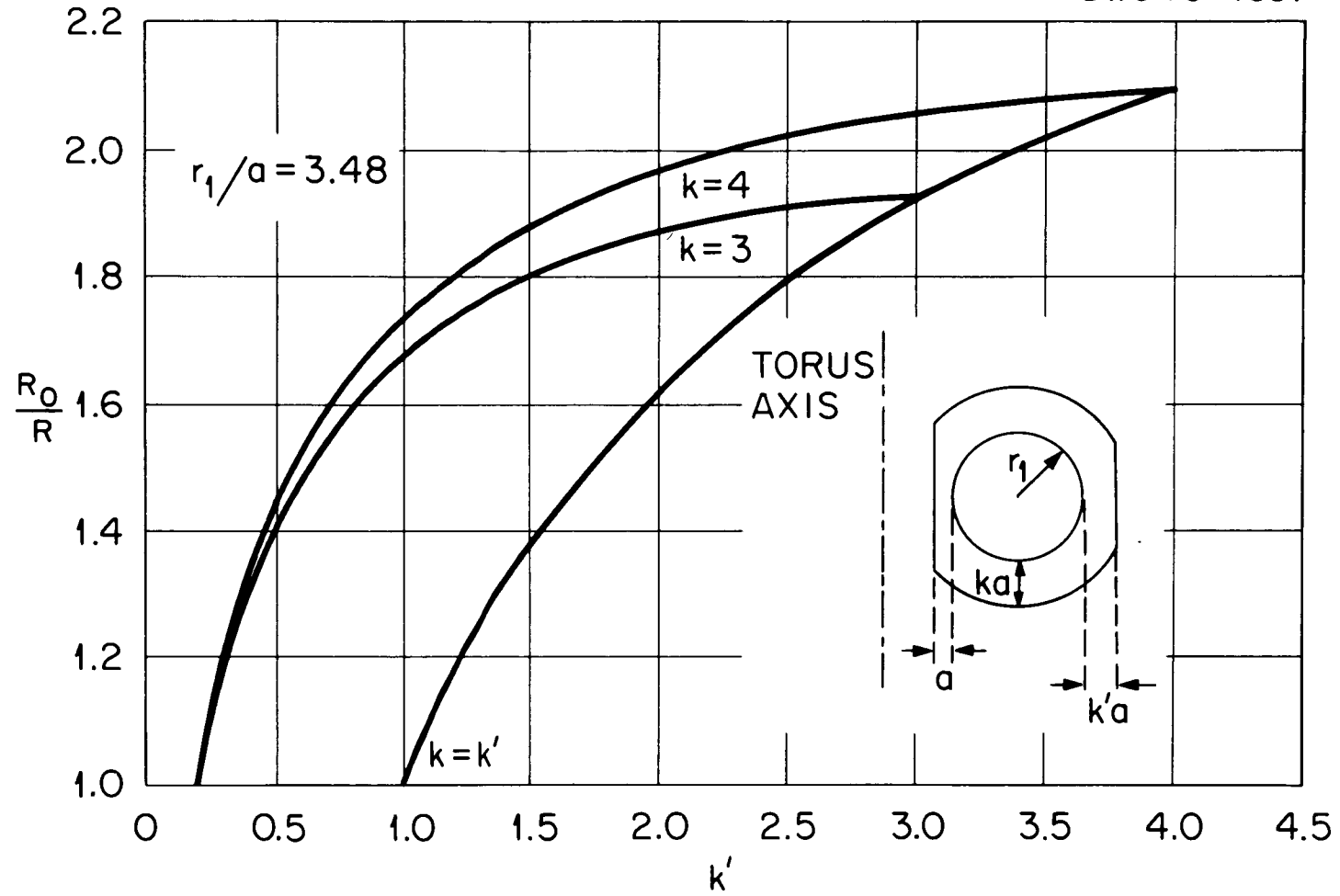
FIGURE 8

ORNL-DWG 72-11627R



Resistance Ratios of Circular Flat End Coils.

FIGURE 9



Resistance Ratios for Double Flat End Coils.

FIGURE 10

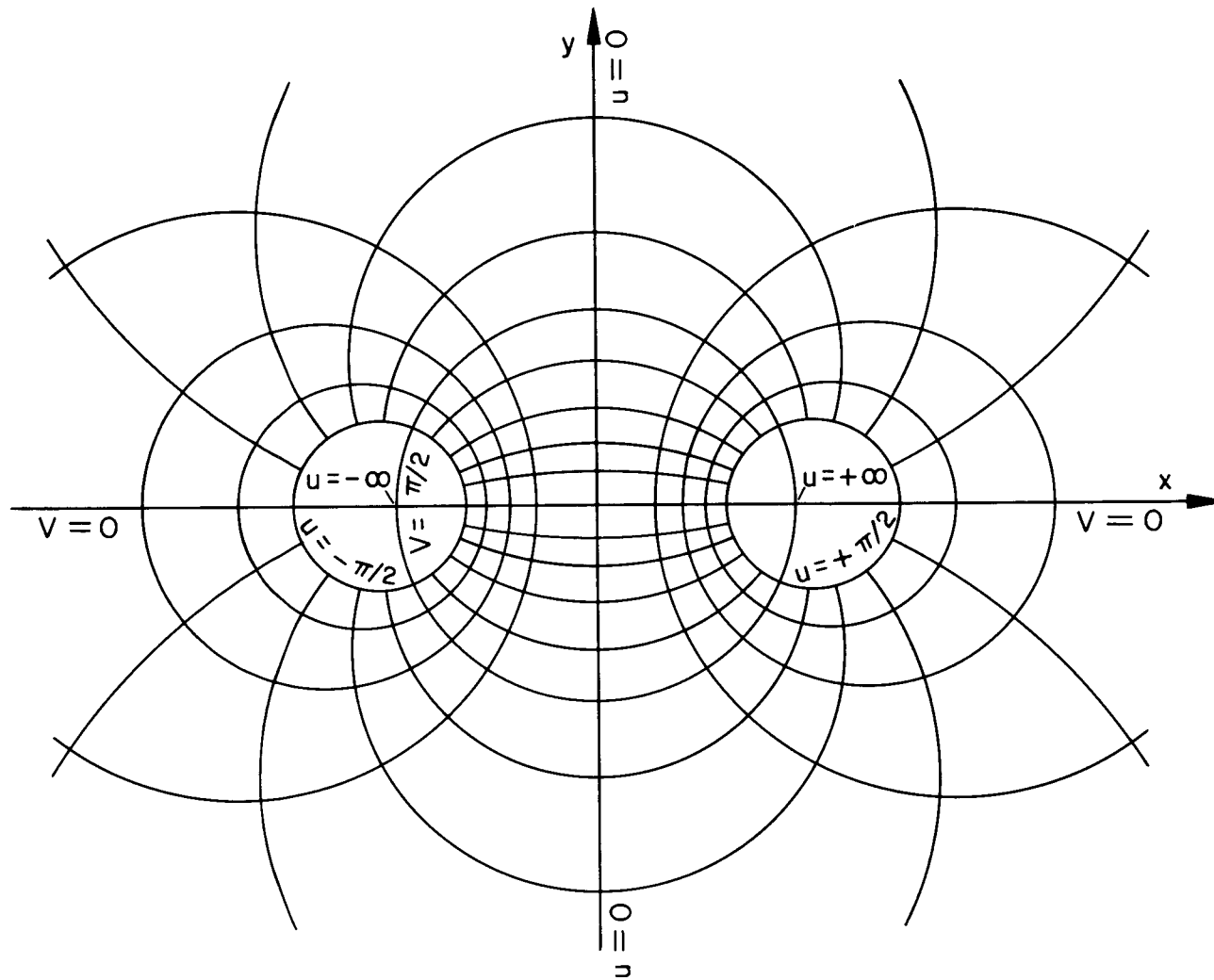


FIGURE 11

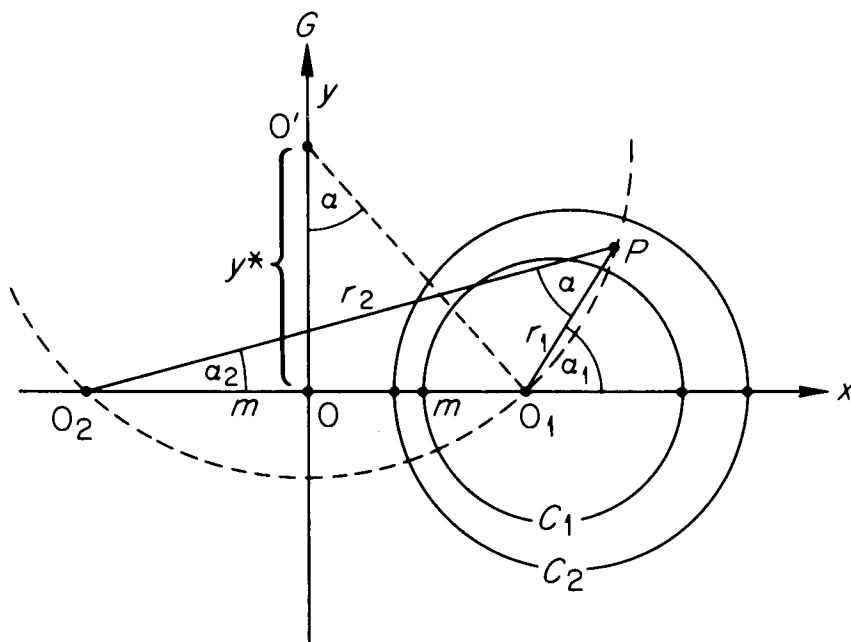


FIGURE 12

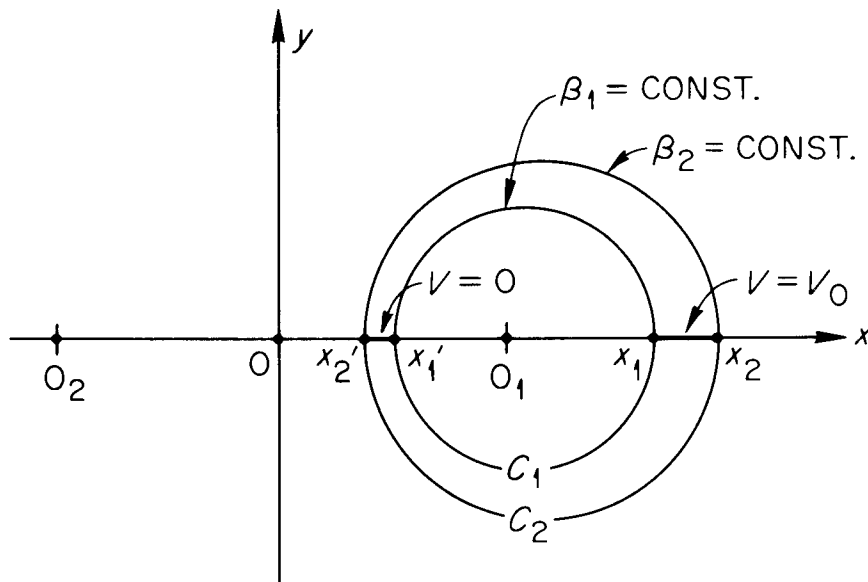
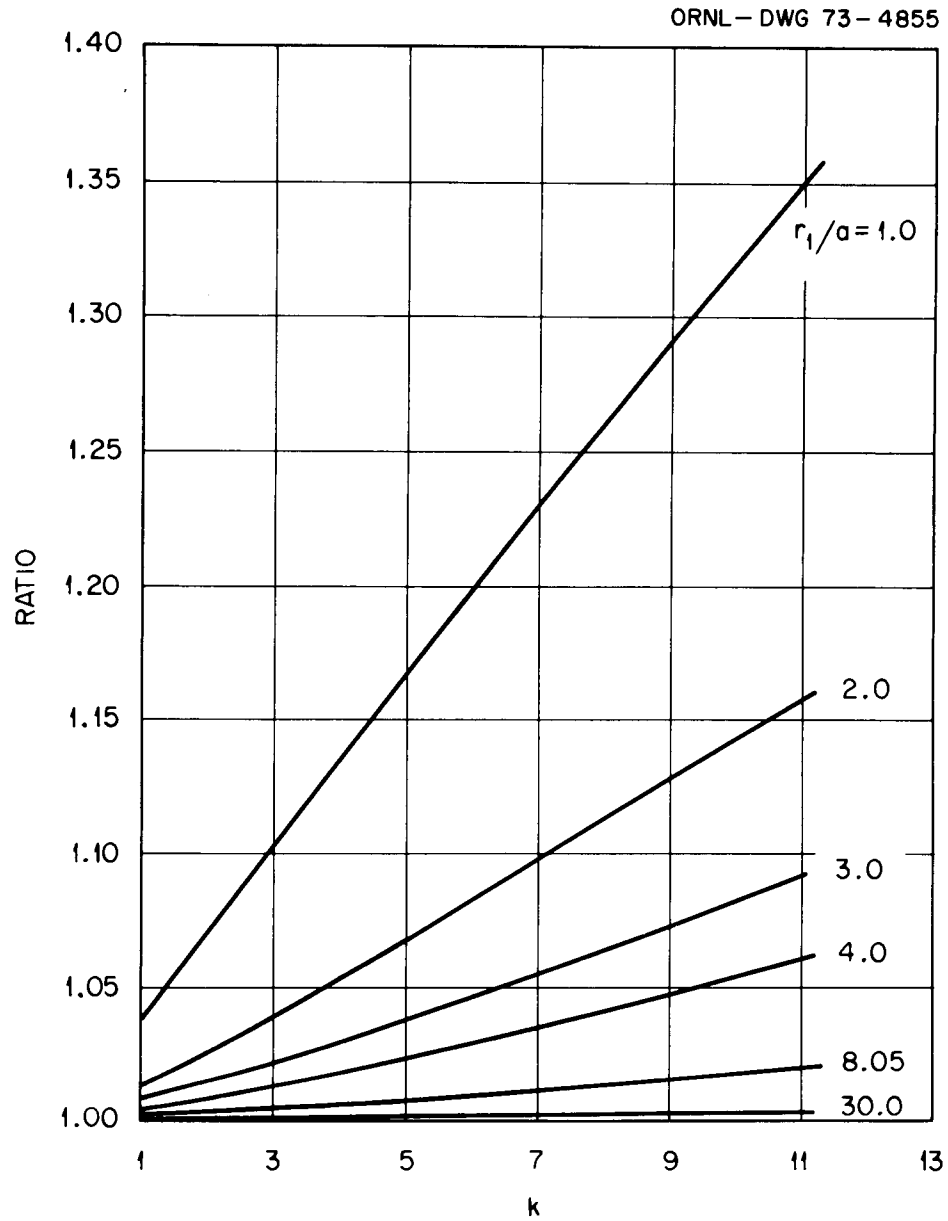


FIGURE 13



Ratio of Resistance Ratios for Circular Eccentric Bitter-Type and Wire-Wound Coils.

FIGURE 14